Supplementary information

ATM activation by transcription- and topoisomerase I-induced DNA double-strand breaks

Olivier Sordet, Christophe Redon, Josée Guirouilh-Barbat, Susan Smith, Stéphanie Solier, Céline Douarre, Chiara Conti, Asako J Nakamura, Benu Brata Das, Estelle Nicolas, Kurt W Kohn, William M Bonner, Yves Pommier

Supplementary Methods

Drugs. The Drug Synthesis and Chemistry Branch, Division of Cancer Treatment, NCI, National Institutes of Health (NIH), provided camptothecin (CPT) and flavopiridol (FLV). Aphidicolin (APD), 5,6-dichlorobenzimidazole 1-β-D-ribofuranoside (DRB), and α-amanitin were obtained from Sigma (St Louis, MO). Hydrogen peroxide (H_2O_2) was obtained from Fisher Scientific (Pittsburgh, PA). Iodouridine (IdU) was obtained from Sigma. The ATM kinase inhibitor (KU55933) (Hickson et al, 2004) and the DNA-PK kinase inhibitor (KU57788) (Leahy et al, 2004) were obtained from Kudos Pharmaceuticals (Cambridge, UK).

Antibodies. Primary antibodies used for microscopy were rabbit anti-53BP1 (NB100-305; Novus, Littleton, CO), mouse anti-ATM-P^{S1981} (4526; Cell Signalling, Beverly, MA), mouse anti-bromodeoxyuridine recognizing also iodouridine (347583; BD Bioscience, San Jose, CA), rabbit anti-Chk2-P^{T68} (2661; Cell Signalling) rabbit anti-fibrillarin (ab5821; Abcam, Cambridge, MA), rabbit anti-GFP (G-1544; Sigma), mouse anti-γ-H2AX (ab18311; Abcam), rabbit anti-γ-H2AX (NB100-384; Novus), rabbit anti-H3K9ac (06-942; Millipore, Billerica, MA), rabbit anti-H3K9me3 (ab8898; Abcam), rabbit anti-MDC1 (ab11169; Abcam), rabbit anti-PML (ab53773; Abcam), mouse anti-PML (sc-966; Santa-Cruz, Santa Cruz, CA), and mouse anti-Pol II-P^{S5} (H14; Covance, Cambridge, MA). Primary antibodies used for immunoblotting were mouse anti-ATM

(sc-23921; Santa-Cruz), mouse anti-ATM-P^{S1981} (4526; Cell Signalling), rabbit anti-ATR (ab2905; Abcam), rabbit anti-Chk2 (2662; Cell Signalling), rabbit anti-Chk2-P^{T68} (2661; Cell Signalling), mouse anti-DNA-PK (NA57; Calbiochem, San Diego, CA), rabbit anti-DNA-PK-P^{S2056} (ab18192; Abcam), mouse anti-DNA-PK-P^{T2609} (ab18356; Abcam), rabbit anti-GAPDH (2118; Cell Signalling), rabbit anti-GFP (G-1544; Sigma), mouse anti-γ-H2AX (ab18311; Abcam), and rabbit anti-H2AX (ab11175; Abcam).

Cell culture. The human peripheral lymphocytes from healthy donors were obtained from the Blood Bank at the NIH and maintained in RPMI 1640 medium supplemented with 10% fetal calf serum. Primary cultures of rat cortical neurons were prepared from E18 rat fetuses. Brains were dissected and dissociated with papain and DNAse I. Neurons were plated in Lab-Tek™ II CC2™ chamber slides (Nalge Nunc Int., Naperville, IL) and maintained in Neurobasal medium supplemented with 1:50 B27 and 1 mM L-glutamine. The human cervical carcinoma HeLa cells were obtained from ATCC (Rockville, MD). The parental human colon carcinoma HCT15 cells and Chk2-complemented HCT15 cells (HCT15-Chk2) were kind gifts from Dr. Chen (Yale University, New Haven, CT) and Dr. Prives (Columbia University, New York, NY). HeLa, HCT15 and HCT15-Chk2 cells were cultured in Dulbecco's modified Eagle's medium supplemented with 10% fetal calf serum.

RNase H1 transfections. HeLa cells were transfected with a plasmid encoding human RNAse H1 tagged with GFP (GFP-RNase H1; a kind gift from Dr. Crouch, NIH, Bethesda, MD) (Cerritelli et al, 2003) or a plasmid encoding GFP alone containing nuclear targeting sequences (GPF-nuc; Invitrogen, Carlbad, CA) using Lipofectamine™ 2000 (Invitrogen) according to the manufacturer's protocol. Experiments were carried out 24 h after transfection. Primary cortical neurons were transfected with GFP-RNase H1 or GPF-nuc using NeuroPORTER™ (Sigma) according to the manufacturer's protocol. Experiments were carried out 72 h after transfection.

Immunofluorescence confocal microscopy. Cytospins of lymphocytes and cultures of neurons and HeLa on Lab-Tek™ II CC2™ chamber slides were processed for

immunofluorescence microscopy. Cells were fixed in 4% paraformaldehyde for 20 min and post-fixed/permeabilized with ice-cold 70% ethanol for 20 min. Cells were incubated with 8% bovine serum albumin (BSA) for 1 h to block non-specific binding before incubation with primary antibodies diluted in 1% BSA/PBS buffer for 1.5 h. After washes, cells were incubated with secondary antibodies (Alexa-488 and/or Alexa-568, Molecular probes, Eugene, OR) diluted in 1% BSA/PBS buffer for 45 min. After washes, cells were incubated with 0.5 mg/ml RNase A and slides were mounted using Vectashield mounting medium (Vector Labs, Burlingame, CA) containing propidium iodide (PI) or 4',6'-diamino-2-phenylindole (DAPI) to counterstained the DNA.

Flow cytometry analyses of γ-H2AX. Lymphocytes were washed with ice-cold PBS, fixed in 4% paraformaldehyde for 10 min at room temperature, and post-fixed/permeabilized with ice-cold 70% ethanol overnight at 4°C. After washes, cells were further permeabilized with 0.25% Triton X-100 for 5 min at 4°C, washed and incubated with the primary mouse anti-γ-H2AX antibody (ab18311; Abcam) (1:250 dilution in 1% BSA/PBS buffer) for 1 h at room temperature. After washes, cells were incubated with the secondary anti-mouse Alexa-488 antibody (Molecular Probes) (1:500 dilution in 1% BSA/PBS buffer) for 30 min at room temperature. Cells were washed and DNA was counterstained with 50 μg/ml propidium iodide (PI) for 10 min in the presence of 0.5 mg/ml RNase A. Fluorescences were monitored on a Becton Dickinson FACScan flow cytometer (BD Bioscience). Percentages of γ-H2AX positive cells were determined using CellQuest software (BD Bioscience).

Cell extracts and immunoblotting. Cell extracts were prepared by lysing cells for 15 min in buffer containing 50 mM Tris-HCl, pH 8.0, 300 mM NaCl, 0.4% NP-40, 10 mM $MgCl_2$ and 5 mM DTT, supplemented with protease inhibitors (Complete; Roche Diagnostics, Indianapolis, IN) and phosphatase inhibitors (50 mM NaF, 1 mM Na_3VO_4, 20 mM β-glycerophosphate). After centrifugation at 10,000 x g for 20 min, supernatants were diluted (v/v) in buffer containing 50 mM Tris-HCl, pH 8.0, 0.4% NP-40 and 5 mM DTT. For detection of H2AX and γ-H2AX (Fig 1E), cell extracts were prepared by lysing cells in buffer containing 1% SDS, 1 mM sodium vanadate, and 10 mM Tris–HCl, pH

7.4, supplemented with protease inhibitors (Complete; Roche Diagnostics) and phosphatase inhibitors (Phosphatase Inhibitor Cocktail 1, Sigma). Viscosity of the samples was reduced by brief sonication. Cell extracts were analysed by immunoblotting as described previously (Sordet et al, 2004).

Neutral COMET assays. Neutral COMET assays in rat cortical neurons were performed according to the manufaturer's instructions (Trevigen, Gaithesburg, MD) except that the electrophoresis was performed at 4°C. DSBs were expressed as relative "comet tail length", which was determined with Adobe Photoshop 7.0 by measuring the number of pixels from the middle of the nucleus to the end of the comet tail.

Uridine incorporation. Lymphocytes (3 x 10^6) were treated with either 10 μM α-amanitin for 17 h, 100 μM DRB for 1 hour or 1 μM flavopiridol for 1 hour before the addition of 20 μCi [5-^{3}H]uridine (PerkinElmer Life Sciences) for 2 h at 37°C. mRNA were isolated using Dynabeads® mRNA DIRECT™ kit according to the manufacturer's instructions (Invitrogen) and radioactivity associated with mRNA was counted by liquid scintillation spectrometry.

Detection of cellular Top1 cleavage complexes (Top1cc). Top1cc were detected using the ICE (*in vivo* complex of enzyme) bioassay (Subramanian et al, 1995). Briefly, cells were lysed in 1% Sarkosyl and homogenized with a Dounce homogenizer. The cell lysates were centrifuged on cesium chloride step gradients at 165,000 x g for 20 h at 20°C. Twenty 0.5-ml fractions were collected and diluted (v/v) into 25 mM potassium phosphate buffer, pH 6.6. The DNA-containing fractions (fractions 7–11) were pooled and applied to polyvinylidene difluoride membranes (Immobilon-P, Millipore) using a slot-blot vacuum manifold. Top1cc were detected by immunoblotting using the C21 Top1 mouse monoclonal antibody (a kind gift from Dr. Yung-Chi Cheng, Yale University, New Haven, CT).

References

Cerritelli SM, Frolova EG, Feng C, Grinberg A, Love PE, Crouch RJ (2003) Failure to produce mitochondrial DNA results in embryonic lethality in Rnaseh1 null mice. *Molecular cell* **11:** 807-815

Hickson I, Zhao Y, Richardson CJ, Green SJ, Martin NM, Orr AI, Reaper PM, Jackson SP, Curtin NJ, Smith GC (2004) Identification and characterization of a novel and specific inhibitor of the ataxia-telangiectasia mutated kinase ATM. *Cancer research* **64:** 9152-9159

Leahy JJ, Golding BT, Griffin RJ, Hardcastle IR, Richardson C, Rigoreau L, Smith GC (2004) Identification of a highly potent and selective DNA-dependent protein kinase (DNA-PK) inhibitor (NU7441) by screening of chromenone libraries. *Bioorg Med Chem Lett* **14:** 6083-6087

Sordet O, Khan QA, Plo I, Pourquier P, Urasaki Y, Yoshida A, Antony S, Kohlhagen G, Solary E, Saparbaev M *et al* (2004) Apoptotic topoisomerase I-DNA complexes induced by staurosporine-mediated oxygen radicals. *J Biol Chem* **279:** 50499-50504

Subramanian D, Kraut E, Staubus A, Young DC, Muller MT (1995) Analysis of topoisomerase I/DNA complexes in patients administered topotecan. *Cancer research* **55:** 2097-2103

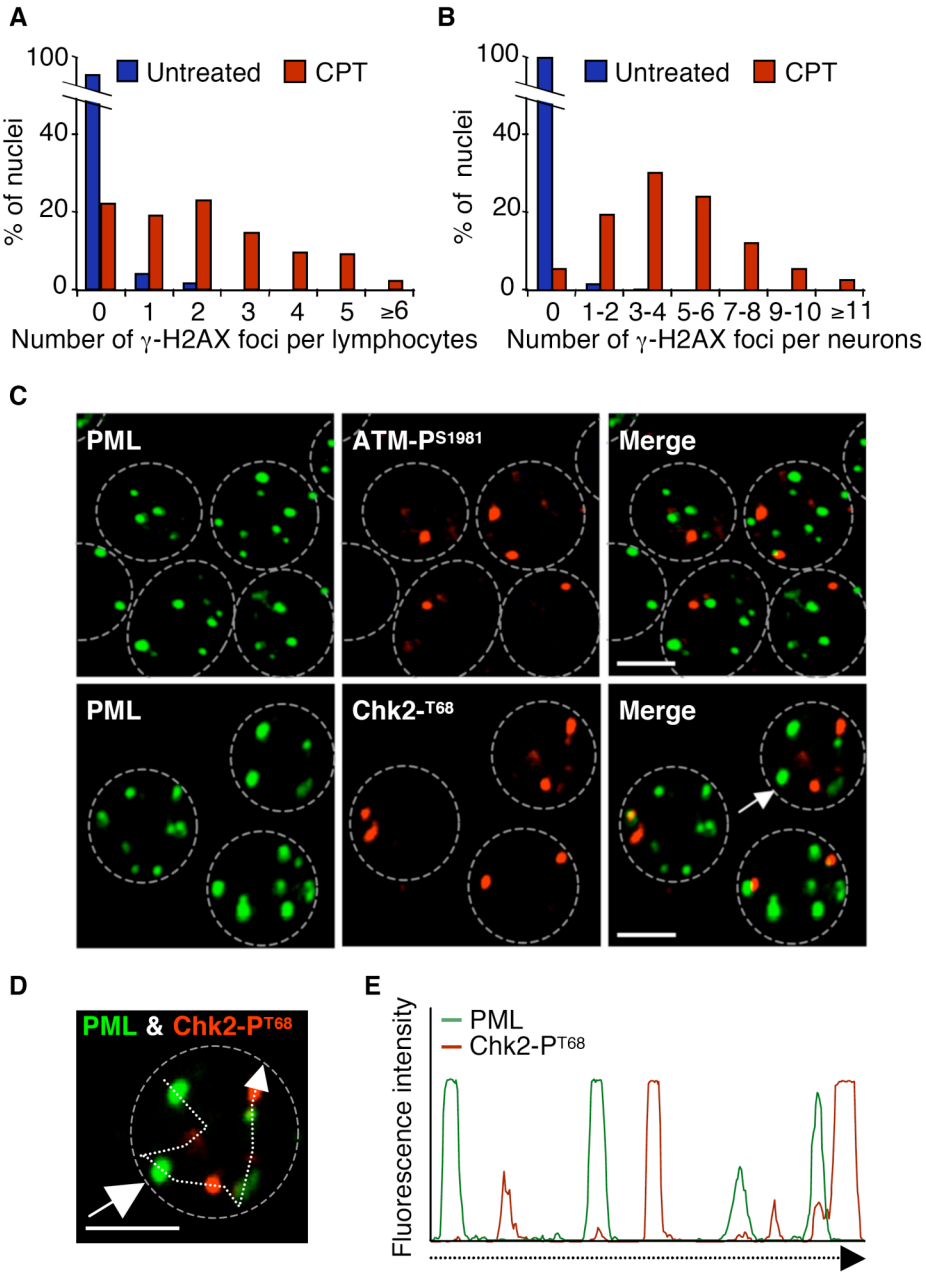

Supplementary Fig S1 | (**A,B**) Distribution of γ-H2AX foci in primary post-mitotic cells in response to CPT. Human lymphocytes (panel A) and rat neurons (panel B) were treated with CPT (25 μM, 1 h). Two hundred nuclei were analyzed. (**C-E**) ATM-P^{S1981} and Chk2-P^{T68} foci do not colocalize with PML nuclear bodies. (**C**) Human lymphocytes were treated with 25 μM CPT for 1 h before staining for PML (green) and either ATM-P^{S1981} (red) or Chk2-P^{T68} (red). Merged images show the absence of colocalization between ATM-P^{S1981} and PML (top panels) and between Chk2-P^{T68} and PML (bottom panels). Bars correspond to 5 μM. Nuclei are outlined with dashed lines. Untreated cells (not shown) displayed similar PML nuclear bodies as CPT-treated cells. (**D**) Magnification of the cell indicated by the arrow in panel C. (**E**) Fluorescence intensities of Chk2-P^{T68} and PML along the dashed line drawn in panel D show the absence of overlapping between the two fluorescences indicating the absence of colocalization.

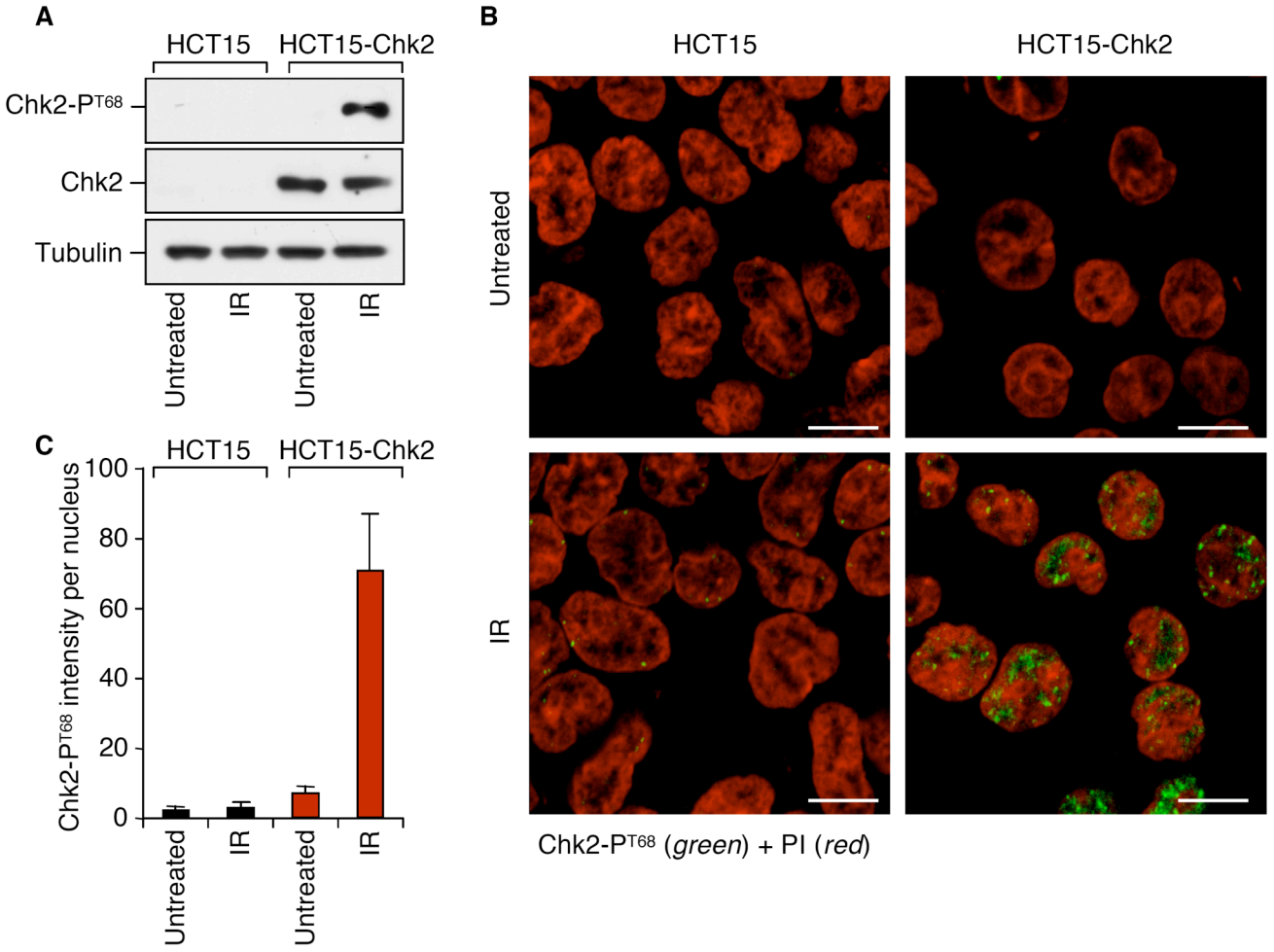

Supplementary Fig S2 | Specificity of the nuclear staining observed with the antibody used against Chk2 phosphorylated at Thr-68 (Chk2-P^{T68}; Cat#2661, Cell Signalling). HCT15 cells (deficient for Chk2) and Chk2-complemented HCT15 cells (referred to as HCT15-Chk2 cells) were exposed to ionizing radiation (IR; 10 Gy in panel A, 3 Gy in panels B and C) and analyzed 30 min post-irradiation. (**A**) Western blotting analyses of Chk2-P^{T68} and total Chk2. Tubulin was used as a loading control. (**B,C**) Cells were stained for Chk2-P^{T68} (green) and DNA was counterstained with propidium iodide (PI, red). Panel B: representative pictures showing that the nuclear staining for Chk2-P^{T68} observed in IR-treated HCT15-Chk2 cells (bottom right) is suppressed in HCT15 cells that are deficient for Chk2 (bottom left). Bars represent 5 μm. Panel C: quantification of Chk2-P^{T68} signal intensity per nucleus (average ± standard deviation).

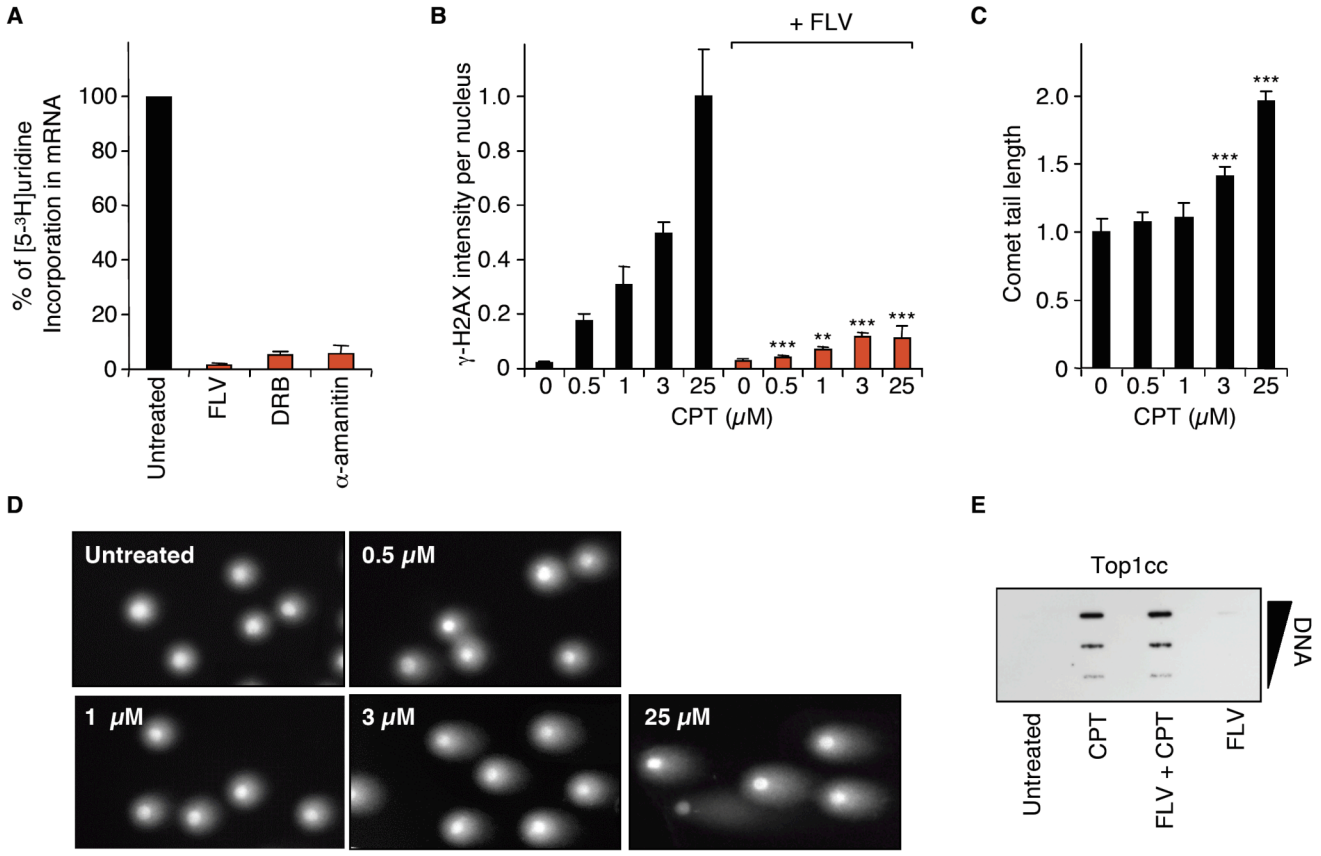

Supplementary Fig S3 | (**A**) Flavopiridol (FLV), 5,6-dichlorobenzimidazole 1-β-D-ribofuranoside (DRB) and α-amanitin inhibit Pol II transcription in post-mitotic human lymphocytes. Cells were treated with FLV (1 μM, 1 h), DRB (100 μM, 1 h) or α-amanitin (10 μM, 17 h) before the addition of 20 μCi [5-^{3}H]uridine for 2 h. Percentages of [5-^{3}H]uridine incorporation in mRNA, which reflect Pol II transcription rate, were normalized to the level of untreated cells, which was taken at 100% (average ± standard deviation). (**B**) Low concentrations of CPT induce FLV-sensitive γ-H2AX in rat neurons. Cells were treated with FLV (1 μM, 1 h) before the addition of CPT (1 h at the indicated concentrations). Cells were then stained for γ-H2AX and DNA was counterstained with propidium iodide (red). γ-H2AX signal intensity per nucleus was quantified following fluorescence microscopy analyses (average ± standard deviation). Asterisks denote significant difference from the CPT-treated cells in the absence of FLV (**, $p<0.01$; ***, $p<0.001$; t-test). (**C,D**) Dose-dependent induction of DSBs by CPT in rat neurons. Cells were treated for 1 h with the indicated concentrations of CPT. Panel C: quantification of the COMET tail length (average ± standard deviation, 40 to 60 cells were examined per group). Asterisks denote significant difference from untreated cells ($p<0.001$; t-test). Panel D: representative pictures of nuclei. (**E**) FLV does not affect the induction of Top1cc by CPT. Human lymphocytes were treated with FLV (1 μM, 1 h) before the addition of CPT (25 μM, 1 h), and Top1cc were detected by slot blot after probing the DNA-containing fractions at three concentrations (10, 3, and 1 μg of DNA) with an antibody against Top1.

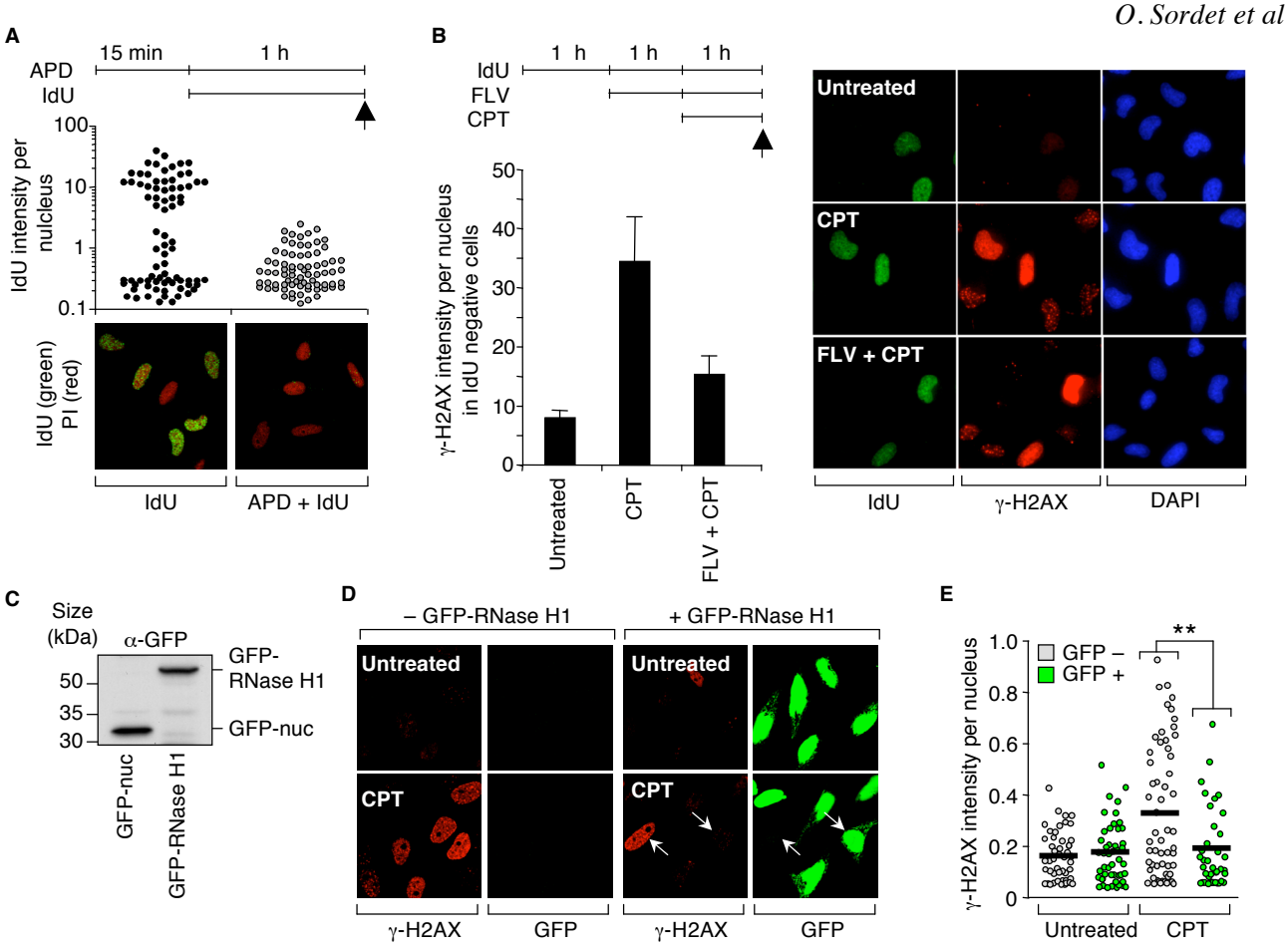

Supplementary Fig S4 | Overexpression of RNase H1 prevents transcription-induced γ-H2AX in HeLa carcinoma cells in response to CPT. (**A**) Aphidicolin (APD) blocks DNA replication in HeLa cells. Top panel: cell treatment protocol. Cells were treated with APD (1 μM, 15 min) before the addition of iodouridine (IdU, 100 μM, 1 h). Arrow indicates sampling time. Cells were then stained for IdU (green) and DNA was counterstained with propidim iodide (PI, red). Lower panel: representative pictures showing that APD suppresses IdU staining indicating DNA replication arrest. Middle panel: distribution of the IdU staining per nucleus. (**B**) Transcription-dependent induction of γ-H2AX in HeLa cells in response to CPT. Top left panel: cell treatment protocol. Cells were treated sequentially with IdU (100 μM), flavopiridol (FLV, 1 μM) and CPT (25 μM) for the indicated times. Cells were then stained for IdU (green) and γ-H2AX (red). DNA was counterstained with DAPI (blue). Arrow indicates sampling time. Right panel: representative pictures showing that CPT induces FLV-dependent γ-H2AX foci in non-replicating cells (IdU negative). Lower left panel: quantification of γ-H2AX signal intensity per nucleus in IdU negative cells (average ± standard deviation). (**C-E**) Overexpression of RNase H1 prevents CPT-induced γ-H2AX in HeLa cells in which replication has been blocked by APD. (**C**) GFP-RNase H1 and GFP alone containing nuclear targeting sequences (GFP-nuc) expression in HeLa cells were detected by Western blotting using an anti-GFP antibody. (**D**) After GFP-RNase H1 transfection, HeLa cells were treated with APD (15 min, 1 μM) before the addition of 25 μM CPT for 1 h. Arrows show that the γ-H2AX labeling (red) and the GFP-RNase H1 labeling (green) are mutually exclusive. Untransfected (– GFP-RNAse H1) and GFP-nuc-transfected cells displayed similar induction of γ-H2AX in response to CPT (not shown). (**E**) Distribution of the γ-H2AX signal intensity per nucleus. HeLa cells were treated as described in panel D. GFP-RNase H1-transfected cells (untreated and CPT-treated) were separated in 2 categories depending on their levels of RNase H1-GFP, which was determined by the intensity of GFP (GFP –: absence or low levels of RNase H1; GFP +: high levels of RNase H1). Black bars mark mean values. Asterisks denote significant difference between the two cell populations (**, $p<0.004$).

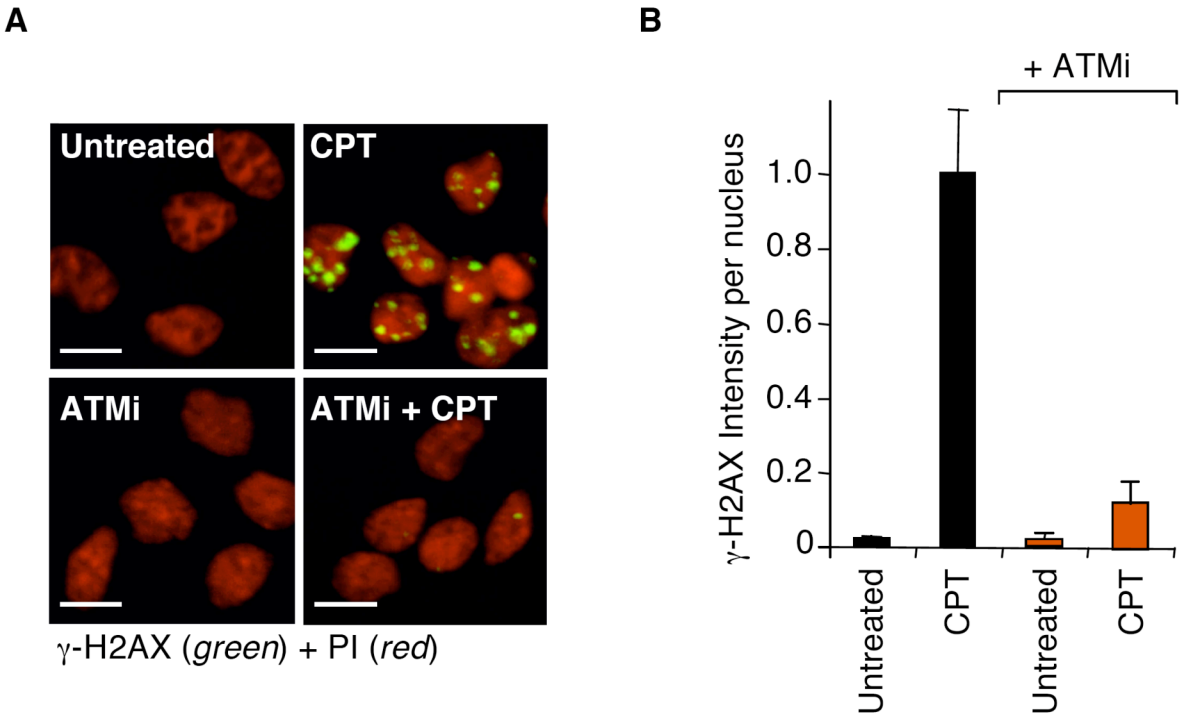

Supplementary Fig S5 | ATM phosphorylates H2AX in post-mitotic neurons in response to transcription-induced DSBs. (**A**) Rat cortical neurons were treated with the ATM kinase inhibitor KU55933 (ATMi, 10 μM) for 1 h before the addition of 25 μM CPT for an additional hour. Cells were stained with γ-H2AX (green) and DNA was counterstained with propidium iodide (PI, red). Bars represent 5 μm. (**B**) Quantification of γ-H2AX signal intensity per nucleus (average ± standard deviation) in neurons treated as described in panel A.

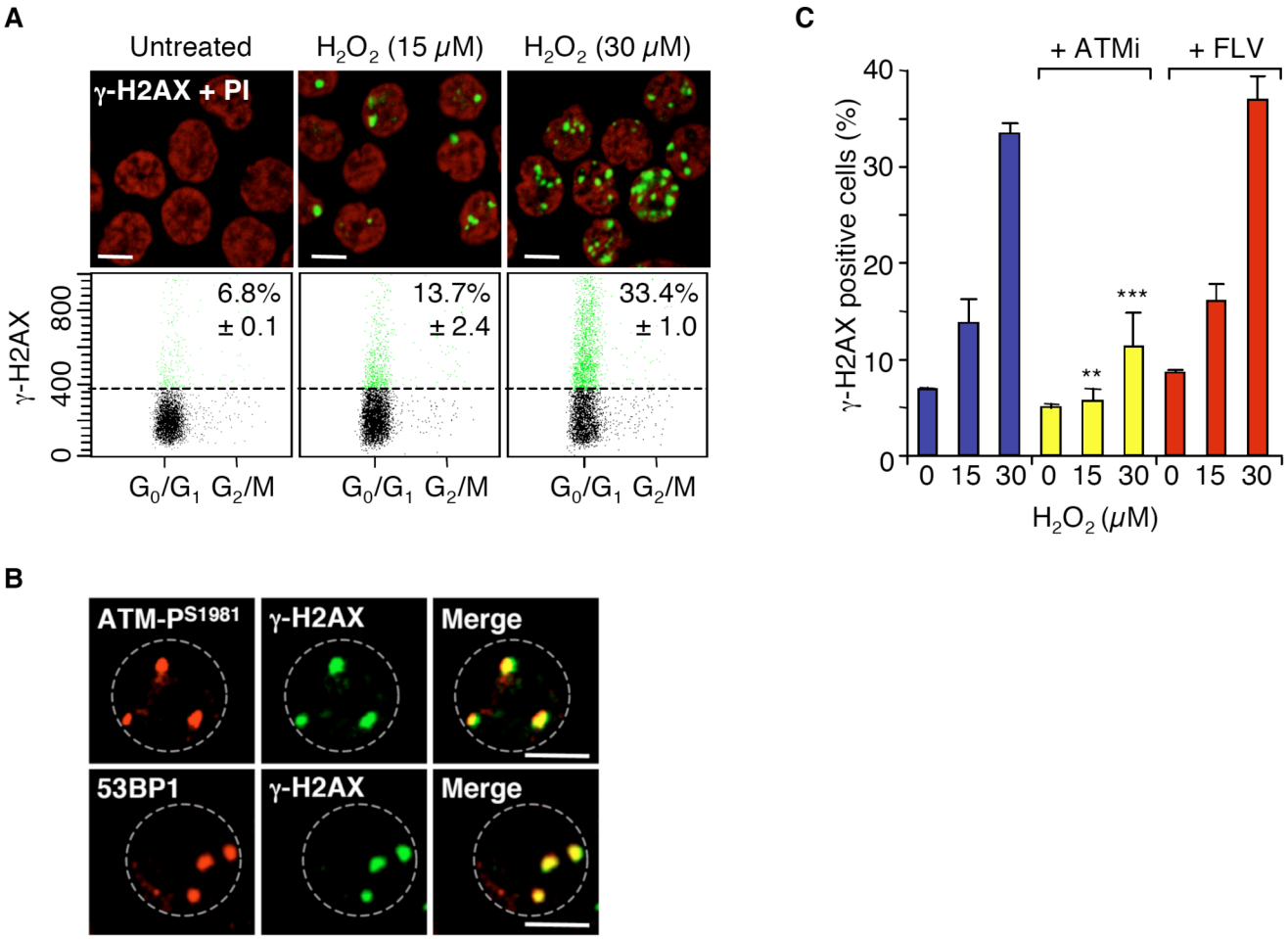

Supplementary Fig S6 | Transcription-independent activation of the ATM pathway in post mitotic cells in response to hydrogen peroxide (H_2O_2). (**A**) Induction of γ-H2AX foci. Cells were treated for 1 h with the indicated concentrations of H_2O_2. Top panels: cells were stained with γ-H2AX (green) and DNA was counterstained with propidium iodide (PI, red). Bars represent 5 μm. Bottom panels: flow cytometry analysis of γ-H2AX and DNA content (PI staining). Numbers indicate percentages of γ-H2AX positive cells (average ± standard deviation), which are shown in green. (**B**) Colocalization of γ-H2AX foci with ATM-P^{S1981} and 53BP1 foci. Human lymphocytes were treated with 15 μM H_2O_2 for 1 h before staining for γ-H2AX (green) and either ATM-P^{S1981} or 53BP1 (red). Images were merged to determine colocalization (yellow). Bars correspond to 5 μm. Nuclei are outlined with dashed lines. (**C**) ATM-dependent and transcription-independent induction of γ-H2AX. Human lymphocytes were treated for 1 h with the ATM kinase inhibitor KU55933 (ATMi, 10 μM; yellow bars) or with the transcription inhibitor flavopiridol (FLV, 1 μM, red bars) before the addition of H_2O_2 for 1 h at the indicated concentrations. Percentages of γ-H2AX positive cells (average ± standard deviation) were determined by flow cytometry as described in panel A. Asterisks denote significant difference from CPT-treated cells in the absence of ATMi (**p<0.01, *** p<0.001; t-test).